

See discussions, stats, and author profiles for this publication at: <https://www.researchgate.net/publication/231634858>

Ground- and Excited-State Proton Transfer in Anthocyanins: From Weak Acids to Superphotoacids

ARTICLE *in* THE JOURNAL OF PHYSICAL CHEMISTRY A · APRIL 2003

Impact Factor: 2.69 · DOI: 10.1021/jp027260i

CITATIONS

32

READS

107

7 AUTHORS, INCLUDING:



Letícia Giestas

New University of Lisbon

9 PUBLICATIONS 250 CITATIONS

SEE PROFILE



Frank Quina

University of São Paulo

164 PUBLICATIONS 4,378 CITATIONS

SEE PROFILE



Antonio Macanita

Technical University of Lisbon

126 PUBLICATIONS 2,424 CITATIONS

SEE PROFILE



João Carlos Lima

New University of Lisbon

143 PUBLICATIONS 2,213 CITATIONS

SEE PROFILE

ARTICLES

Ground- and Excited-State Proton Transfer in Anthocyanins: From Weak Acids to Superphotoacids

Paulo F. Moreira, Jr.,[†] Leticia Giestas,[‡] Chang Yihwa,[†] Carolina Vautier-Giongo,[†]
Frank H. Quina,[†] Antonio L. Maçanita,^{‡,§} and João C. Lima^{*,#}

Instituto de Química, Universidade de São Paulo, São Paulo, Brazil, Instituto de Tecnologia Química e Biológica, Oeiras, Portugal, Departamento de Química, Instituto Superior Técnico, Lisbon, Portugal, and Centro de Química Fina e Biotecnologia, Departamento de Química, Faculdade de Ciências e Tecnologia, Universidade Nova de Lisboa, Lisbon, Portugal

Received: October 21, 2002; In Final Form: March 28, 2003

Malvidin-3,5-diglucoside (malvin), cyanidin-3,5-diglucoside (cyanin), and pelargonidin-3,5-diglucoside (pelargonin) are among the most representative anthocyanins because of their abundance in the most common red flowers and fruits. Anthocyanin color is directly affected by the pH-dependent chemistry of the red (acid) form of these compounds, while anthocyanin photostability is a function of the photophysics of the first excited singlet state. In the present work, we employ laser flash photolysis and picosecond time-correlated single-photon counting to determine the dynamics of the proton-transfer reactions of these three anthocyanins in the ground [deprotonation rate constants, $k_d = 1.3 \times 10^6 \text{ s}^{-1}$ (pelargonin), $1.8 \times 10^6 \text{ s}^{-1}$ (cyanin), and $3.8 \times 10^6 \text{ s}^{-1}$ (malvin)] and first excited singlet state [deprotonation rate constants, $k_d = 4.3 \times 10^{10} \text{ s}^{-1}$ (pelargonin), $4.0 \times 10^{10} \text{ s}^{-1}$ (cyanin), and $1.6 \times 10^{11} \text{ s}^{-1}$ (malvin)], respectively. The ground- and excited-state proton-transfer rate constants for anthocyanins and for photoacids of the naphthol type are found to correlate with an empirical parameter related to the ionic character of the dissociable OH bond. The present results show that the typically weak fluorescence of the flavylum cation form of anthocyanins is due primarily to competitive ultrafast, adiabatic proton transfer to water. This process is highly efficient as an energy-wasting mechanism, as would be required by an *in vivo* role such as protection of plant tissues from potentially deleterious excess radiant energy.

Introduction

Malvin, cyanin, and pelargonin (Scheme 1) are among the most representative anthocyanins because of their abundance in the most common red flowers and fruits.^{1,2} The use of anthocyanins as food pigments² or potential antioxidants^{3,4} and the incredible richness of their chemistry in both the ground^{5–9}

and excited states^{10–14} are motives for general interest in these compounds.

The fate of the green-wavelength solar light absorbed *in vivo* and *in vitro* by anthocyanins is presently unknown. In particular, there are very few studies of the excited-state deactivation mechanisms,¹⁵ including photochemistry,^{16,17} of this class of compounds. On the other hand, synthetic flavylum ions (Scheme 1) are superphotoacids, and time-resolved fluorescence measurements have shown that ultrafast excited-state proton transfer to water is the dominant process that occurs upon excitation of synthetic anthocyanin analogues such as 4-methyl-

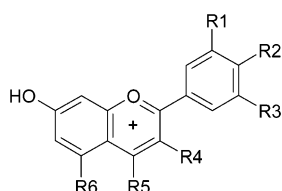
[†] Universidade de São Paulo.

[‡] Instituto de Tecnologia Química e Biológica.

[§] Instituto Superior Técnico.

[#] Universidade Nova de Lisboa.

SCHEME 1

HMF: R1=R2=R3=R4=R6=H; R5=CH₃

DHF: R1=R3=R4=R5=R6=H; R2=OH

Pelargonin: R1=R3=R5=H; R2=OH; R4=R6=Glucosyl

Cyanin: R3=R5=H; R1=R2=OH; R4=R6=Glucosyl

Malvin: R5=H; R1=R3=OCH₃; R2=OH; R4=R6=GlucosylOenin: R5=H; R1=R3=OCH₃; R2=R6=OH; R4=Glucosyl

7-hydroxyflavylium^{10,18} chloride (HMF) and 4',7-dihydroxyflavylium¹⁸ chloride (DHF) in aqueous solution.

The ground-state prototropic reactions of the red form of anthocyanins (the flavylium cation, Scheme 1) are also important because they directly affect anthocyanin color. Nonetheless, until recently, kinetics of these reactions had not been directly determined for any of the anthocyanins or anthocyanin analogues, in large part because the rates fall in a time range (microseconds) that is inaccessible by conventional stopped-flow techniques. By using laser flash photolysis to perturb the ground-state acid–base equilibrium, we demonstrated¹⁹ that both the deprotonation and reprotonation rate constants of synthetic flavylium salts (HMF, DHF) and of the natural anthocyanin malvidin-3-glucoside (oenin) could be readily determined.

Because the perturbation of the ground-state acid–base equilibrium is a direct consequence of excited-state proton transfer (ESPT), the laser flash photolysis results with oenin also provided the first evidence, albeit indirect, for the occurrence of excited-state proton transfer in a naturally occurring anthocyanin.¹⁹ Unlike HMF and DMF, for which direct evidence for ESPT can be readily obtained from fluorescence measurements, monoglucosylated anthocyanins such as oenin are practically nonfluorescent (fluorescence quantum yields, ϕ_f , typically smaller than 4×10^{-3}).²⁰

Diglucosylated anthocyanins such as malvidin-3,5-diglucoside (malvin), cyanidin-3,5-diglucoside (cyanin), and pelargonidin-3,5-diglucoside (pelargonin) exhibit slightly higher fluorescence quantum yields than their monoglucosylated analogues. In this work, we demonstrate that these three natural anthocyanins also undergo ultrafast proton transfer to water in the excited state and analyze the kinetics of proton transfer in both the ground and excited states.

Experimental Section

Materials and Sample Preparation. Pelargonin, cyanin, and malvin chlorides (HPLC-purified) were purchased from Extrasynthèse and used as received. Water was distilled twice and deionized (Elgastat UHQ PS or Millipore Milli-Q purification system). The concentration of the flavylium chlorides was typically ca. 10^{-5} M. For pH values above 2, the pH was adjusted with 24 mM phosphate buffers and measured at 20 °C with a Crison micropH 2002. Below pH 2, the desired hydrogen ion concentration was obtained by exact dilution of commercial perchloric acid (Riedel-de-Haen, PA 60%). UV–vis absorption spectra were recorded on a Beckman DU-70, a Hewlett-Packard 8452A diode array, or a Shimadzu UV-2510 PC UV–vis recording spectrophotometer. Steady-state fluorescence spectra were recorded on a SPEX F212I Fluorolog or a SPEX-Jobyn Yvon Fluorolog 3 spectrofluorimeter. All fluorescence spectra are corrected. Fluorescence quantum yields were obtained using the fluorescein dianion in 0.01 M aqueous NaOH ($\phi_f = 0.90$)²¹ as standard.

Laser Flash Photolysis. The laser flash photolysis experiments were carried out with an Edinburgh Analytical Instru-

ments LP900 laser flash photolysis system as previously described.⁵ Excitation was carried out with the second harmonic (532 nm) of a Surelite I-10 Nd:YAG laser. Solutions were stirred between each laser shot, and 10 laser shots were averaged to obtain the transient absorption decays. The decays were analyzed using the Edinburgh Analytical Instruments LP900 system software. Lifetimes shorter than 30 ns were deconvoluted using the pulse shape of the laser (obtained by monitoring the Raman scattering peak of water in the fluorescence mode of the LP900). Because the transient lifetime was wavelength-independent, transient absorption spectra were obtained by plotting the preexponential coefficients of the decays (or recoveries) at each wavelength.

Time-Resolved Fluorescence. Fluorescence decays were measured using the time-correlated single-photon counting technique as described elsewhere.¹⁰ Alternate measurements (10^3 counts at the maximum per cycle) of the excitation pulse profile and sample emissions were made until approximately 5×10^3 total counts had been accumulated at the maximum. Fluorescence decays were deconvoluted from the excitation pulse using G. Striker's Sand program, which permits individual and global analysis of the decays.²²

Semiempirical Calculations. 1. Basic Procedure. The geometries were optimized using MM⁺ molecular mechanics with point charges.²³ The charges were calculated by single-point calculations with the semiempirical AM1 method at the RHF level with configuration interaction (99 singly excited configurations). The process was repeated iteratively until the MM⁺ geometries and AM1 atomic charges were invariant.

2. Control Procedure. Optimized geometries were obtained for the ground states using AM1 and PM3 at the RHF and UHF levels. Single-point calculations were then performed with and without configuration interaction. The atomic charges and O–H distances obtained by each procedure were used to calculate E_{ionic} . In all cases, a correlation similar to that in Figure 7 was obtained, though the absolute values of the points changed slightly depending on the method. For simplicity, results obtained by the basic procedure are reported here. In the case of the polyhydroxylated anthocyanins, the values for the most acidic hydroxyl group (less negatively charged oxygen) were used in the correlation. For compounds in which intramolecular H-bonded conformations are possible (e.g., 1-naphthol-2-sulfonate, 2-naphthol-3,6-disulfonate), the average of the charges of the H-bonded and non-H-bonded conformations was used.

Results

Steady-State and Time-Resolved Fluorescence. Figure 1 shows the absorption and fluorescence emission spectra of the natural anthocyanin pelargonidin-3,5-diglucoside (pelargonin, Figure 1c), together with those of the synthetic flavylium salts 4-methyl-7-hydroxyflavylium chloride (HMF, Figure 1a) and 4',7-dihydroxyflavylium chloride (DHF, Figure 1b) in aqueous solution at pH 1. Figure 1a,b also shows the emission spectra, under the same conditions, of the methoxy analogues of HMF

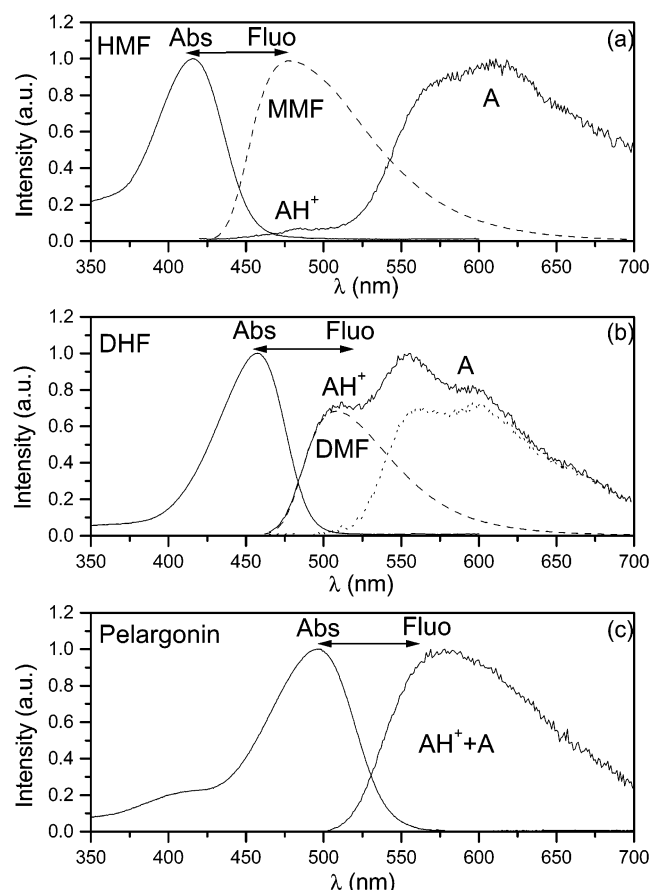


Figure 1. Absorption and fluorescence spectra (solid curves) of 10^{-5} M aqueous solutions of (a) HMF, (b) DHF, and (c) pelargonidin-3,5-diglucoside at pH 1. The dashed lines in panels a and b correspond to the fluorescence of the methoxylated analogues, MMF and DMF, under the same conditions. The dotted line in panel b is the emission of the quinonoidal base, A, of DHF at pH 6.

and DHF, that is, 4-methyl-7-methoxyflavylium chloride (MMF) and 4',7-dimethoxyflavylium chloride (DMF), neither of which can deprotonate.

Compared to the methoxy analogues, the fluorescence spectra of the synthetic flavylium salts HMF and DHF show a strong reduction in the intensity of emission from the excited acid form, $(\text{AH}^+)^*$ ($I_{\text{MMF}}/I_{\text{HMF}} \approx 500$ at $\lambda_{\text{em}} = 480$ nm and pH = 1 and $I_{\text{DMF}}/I_{\text{DHF}} \approx 44$ at $\lambda_{\text{em}} = 510$ nm and pH = 1).²⁰ Moreover, even though the flavylium cation is the only form present in the ground state at this pH, the emission of the excited base form, A^* , is clearly visible. Thus, fluorescence spectral identification of ESPT is quite straightforward in these compounds.^{10,18} In contrast, the fluorescence spectrum of pelargonin at pH 1 exhibits only a broad emission band and no clear spectral evidence for ESPT. The emission spectra of the other two natural anthocyanins, cyanin and malvin at pH 1, are similar to that of pelargonin.

Figure 2 shows normalized emission spectra of pelargonin, cyanin, and malvin in water at higher proton concentrations, ranging from 0.11 to 2.62 M. Increasing the proton concentration produces two effects: (1) the emission spectra narrow somewhat, reflecting a decrease in the emission intensity on the higher wavelength side of the band, and (2) the fluorescence intensity at the maximum increases (see insets). On the other hand, the absorption spectra of the three anthocyanins do not change in this proton concentration range. These observations indicate that the broad emission band observed at pH 1 consists, in reality, of two strongly overlapping emission bands ascribable to the

TABLE 1: Decay Times of Pelargonin, Cyanin, and Malvin in Aqueous Solution at 20 °C

compound	$[\text{H}^+]$ (M)	λ_{em} (nm)	τ_1 (ps)	τ_2 (ps)	a_1	a_2	χ^2
pelargonin	0.009	510	118.3	23.1	0.12	0.88	1.21
	1.0	510	217	7.6	0.31	0.69	1.14
cyanin	0.009	571	111.9	24.9	0.60	0.40	1.20
	0.03	571	112.2	20.0	0.55	0.45	1.07
malvin	1.0	571	137.4	10.0	0.19	0.81	0.99
	0.03	560	19.5	5.4	0.36	0.64	1.53
	2.62	560	31.9	2.4	0.12	0.88	2.50
	9.14	560	38.2	0.8	0.05	0.95	2.48

excited acid, $(\text{AH}^+)^*$, and base, A^* , forms of the natural anthocyanins, the base emitting at the longer wavelengths.

Figure 3 shows the fluorescence decays of pelargonin measured at the onset (510 nm) and at the red edge of the emission band (650 nm) in aqueous solution at pH 1, at which only the acid form is present in the ground state. At both wavelengths, the decays are biexponential with a shorter decay time of $\tau_2 = 20$ ps and a longer decay time of $\tau_1 = 124$ ps. The preexponential coefficient associated with the shorter decay time (a_2) changes sign from positive to negative with increasing emission wavelength, clearly indicating the presence of a species formed in the excited state that emits at the red edge of the spectrum. This species is identified as the excited base, A^* . In Figure 4, the values of the two decay times of pelargonin in water are plotted as a function of the hydrogen ion concentration, $[\text{H}^+]$.

The fluorescence decays of cyanin and malvin (not shown) are also biexponential with lifetimes that show a similar dependence on $[\text{H}^+]$ (Table 1). However, in the case of malvin, the decay times are much shorter. For instance, τ_2 of malvin is 5.4 ps at pH = 1.5 and decreases to a value of less than 1 ps (below the experimental resolution of the apparatus) at $[\text{H}^+] = 9.14$ M. The fit of the decays as the sum of two exponentials was poor and did not improve upon increasing the number of exponentials, a problem that is probably related to the unresolved short decay time.

Flash Photolysis. Laser flash photolysis was previously employed to measure the rate constants for deprotonation of the ground state of the flavylium cation and for reprotonation of the quinonoidal base of HMF, DMF, and oenin in water¹⁹ and of oenin²⁴ and HMF²⁵ in anionic sodium dodecyl sulfate (SDS) micelles. This method takes advantage of the fact that both the deprotonation of the flavylium cation in the singlet excited state (5–30 ps) and the decay of the excited base to its ground state (130–250 ps) are subnanosecond processes. Thus, under these conditions, the 5 ns laser pulse in effect shifts the *ground state* acid–base equilibrium toward the base within the pulse duration.¹⁹

A differential absorption spectrum of the transient produced in an aqueous solution of cyanin at pH 2, measured immediately after the laser pulse, is shown in Figure 5. The spectrum shows a depletion at the absorption maximum of the acid, AH^+ (ca. 500 nm), and an increase in absorbance at ca. 560 nm due to the quinonoidal base, A, as found for oenin in water.¹⁹ Similar observations (depletion at the absorption maximum of the acid and enhanced absorption at higher wavelengths due to quinonoidal base formation) were made for pelargonin and malvin and constitute additional evidence for the occurrence of ESPT from the three anthocyanins in aqueous solution.

The relaxation of the three anthocyanins back to equilibrium in the ground state was followed with nanosecond time resolution by monitoring either the disappearance of the quinonoidal base or the recovery of flavylium cation. For all three anthocyanins, the decay of the absorption of A (at ca. 600

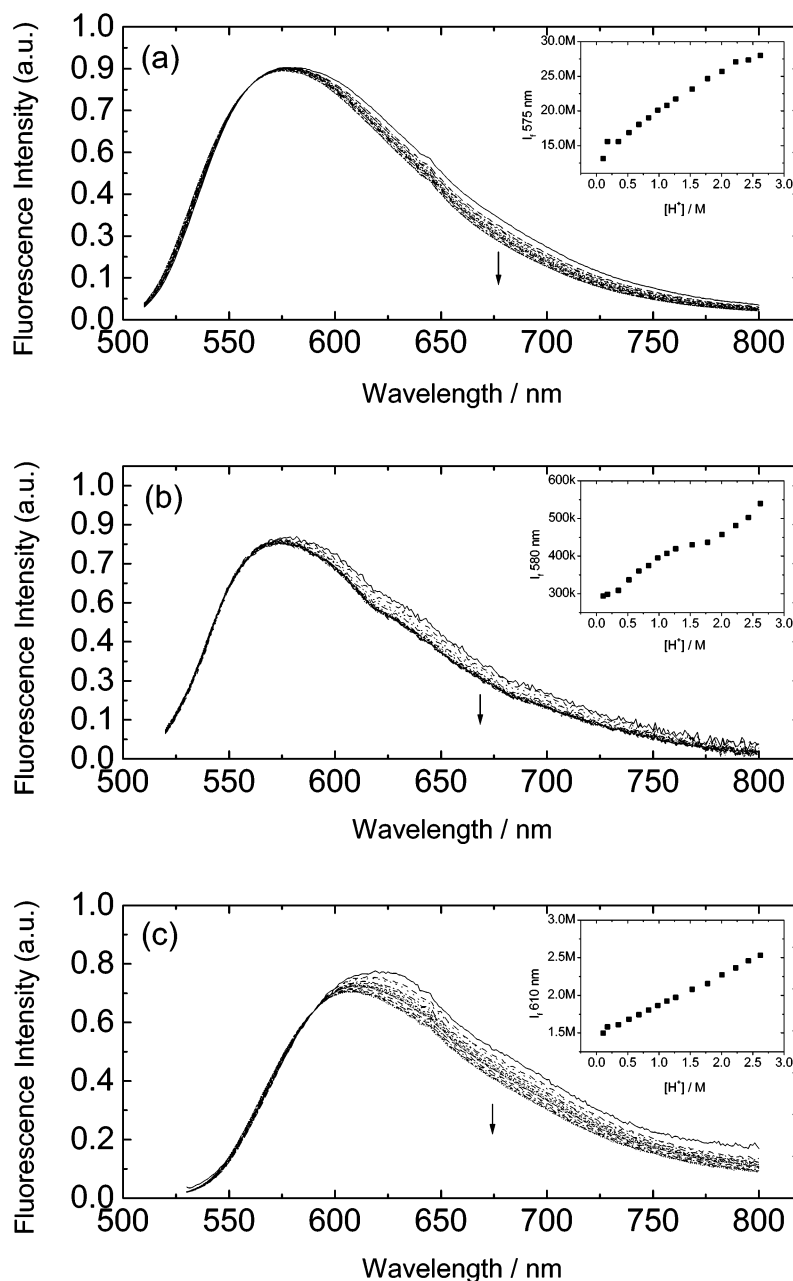


Figure 2. Emission spectra in water at $[H^+] = 0.11, 0.18, 0.35, 0.52, 0.68, 0.83, 0.98, 1.13, 1.27, 1.53, 1.78, 2.01, 2.23, 2.43,$ and 2.62 M of (a) pelargonin ($\lambda_{\text{exc}} = 490$ nm) normalized at $\lambda_{\text{em}} = 560$ nm, (b) cyanin ($\lambda_{\text{exc}} = 510$ nm) normalized at $\lambda_{\text{em}} = 560$ nm, and (c) malvin ($\lambda_{\text{exc}} = 520$ nm) normalized at $\lambda_{\text{em}} = 590$ nm. The arrows denote the region in which the emission decreases with increasing $[H^+]$.

nm) and the recovery of AH^+ (at ca. 500 nm) were single exponentials with identical lifetimes. The decay times increase with increasing pH, as previously observed¹⁹ for oenin and for the synthetic flavylum salts HMF and DHF.

Discussion

Ground-State Proton Transfer. As shown before for HMF, DMF, and oenin, the ground-state proton-transfer rate constants can be evaluated via nanosecond laser flash photolytic perturbation of the position of the ground-state acid–base equilibrium. The reciprocal of the decay time (k_{obs}) of the transient is related to the deprotonation (k_d) and protonation (k_p) rate constants by eq 1, which predicts a linear dependence of k_{obs} on the proton concentration.

$$k_{\text{obs}} = k_d + k_p[H^+] \quad (1)$$

Figure 6 shows the linear plots of k_{obs} as a function of $[H^+]$ obtained for the three anthocyanins, pelargonin, cyanin, and malvin. From the intercepts and slopes of these plots, the deprotonation rate constants of AH^+ and the protonation rate constants of A were obtained (Table 2). As found for HMF, DHF, and oenin, the protonation of the base form, A, is diffusion-controlled. Although the deprotonation rate constant of AH^+ is obtained with a large error,¹⁹ it is interesting to note that the value of k_d appears to increase with the number of hydroxyl or methoxy groups attached to the chromophore of the anthocyanin.

Excited-State Proton Transfer. The flash photolysis results and the steady-state and time-resolved fluorescence data demonstrate the occurrence of ESPT for the three natural anthocyanins. Kinetic analysis of the data is not trivial²⁶ because the experimental preexponential coefficients cannot be utilized

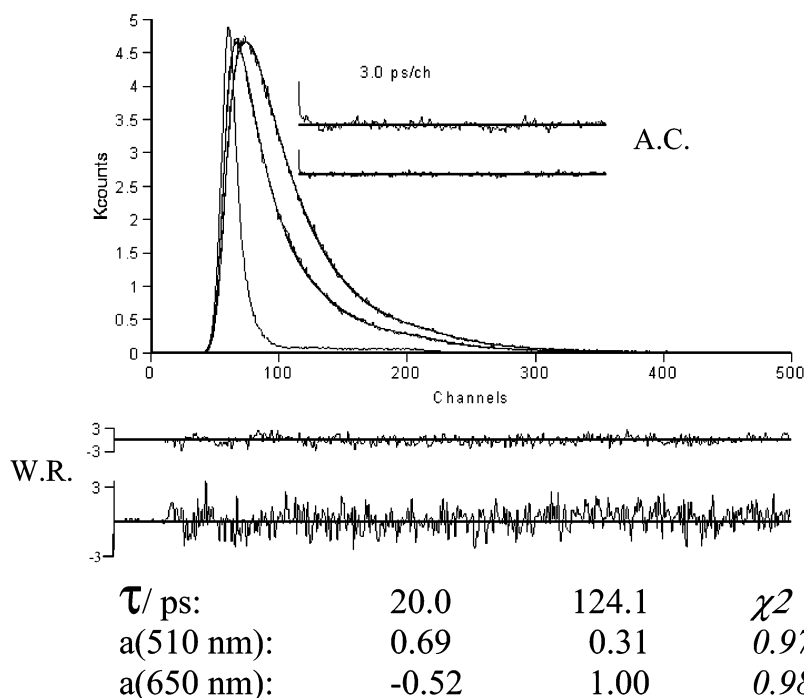


Figure 3. Global analysis of the fluorescence decays of pelargonidin-3,5-diglucoside at $\lambda_{\text{em}} = 510$ nm and $\lambda_{\text{em}} = 650$ nm at pH = 1 ($\lambda_{\text{exc}} = 465$ nm). Weighted residuals (WR) and autocorrelation functions (AC) are also plotted.

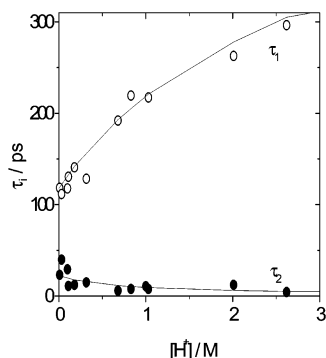


Figure 4. Plot of the decay times of pelargonin as a function of $[\text{H}^+]$; lifetimes obtained by global analysis of the fluorescence decay in water at 510 and 650 nm.

because the emission spectra of the excited acid, $(\text{AH}^+)^*$, and base, A^* , forms strongly overlap. Under these conditions, the experimental preexponentials are linear combinations of the true preexponentials of the decays of $(\text{AH}^+)^*$ and A^* at all wavelengths.

Nonetheless, the pH dependence of the two decay times, τ_1 and τ_2 in Figure 4, does provide some useful information. The longest decay time, τ_1 , increases with increasing $[\text{H}^+]$, which is opposite to the trend of τ_1 usually found in other acid–base systems. At low $[\text{H}^+]$, at which the back-protonation of A^* can be neglected, τ_1 tends to a value equal to the quinonoidal base lifetime ($\tau_1 = 118$ ps at $[\text{H}^+] = 0.009$ M), corresponding to $k_{\text{A}} = 8.5 \times 10^9 \text{ s}^{-1}$. At sufficiently high proton concentrations (9.14 M perchloric acid), the back-protonation rate should exceed 10^{11} s^{-1} (assuming $k_{\text{p}}^* \approx 10^{10} \text{ M}^{-1} \text{ s}^{-1}$)¹⁹ and the kinetics enter the so-called fast-equilibrium regime,²⁷ in which the forward and back reaction rates are much larger than the reciprocal lifetimes of $(\text{AH}^+)^*$ and A^* ($k_{\text{d}}^*, k_{\text{p}}^*[\text{H}^+] \gg k_{\text{AH}^+}, k_{\text{A}}$).²⁵ In the limit of $k_{\text{p}}^*[\text{H}^+] \gg k_{\text{d}}^*$, the value of τ_1 is equal to the flavylium cation lifetime ($\tau_1 = 540$ ps at $[\text{H}^+] = 9.14$ M), corresponding to $k_{\text{AH}^+} = 1.85 \times 10^9 \text{ s}^{-1}$.

The short decay time, τ_2 , decreases with increasing $[\text{H}^+]$. At low $[\text{H}^+]$, where the reprotonation process becomes unimportant, τ_2 levels off at a relatively constant value of 23 ps, which should in turn be equal to $1/(k_{\text{d}} + k_{\text{AH}^+})$. Because the flavylium cation lifetime is much longer ($\tau_{\text{AH}^+} = 1/k_{\text{AH}^+} = 540$ ps), $\tau_2 = 23$ ps is quite close in magnitude to the value of $1/k_{\text{d}}$. From $k_{\text{d}} = 1/\tau_2 - k_{\text{AH}^+}$, one obtains $k_{\text{d}} = 4.2 \times 10^{10} \text{ s}^{-1}$. The values of the deprotonation rate constants, k_{d} , for the three anthocyanins, obtained from the reciprocal of the shortest decay time at pH ≥ 2 , are presented in Table 2. In the case of malvin, the value of τ_2 at pH 1.5 was used because ground-state hydration of the flavylium cation prevails at pH ≥ 2 .

The highest value of the excited-state deprotonation rate constant was found for malvin ($k_{\text{d}} = 1.6 \times 10^{11} \text{ s}^{-1}$), which is very close to the Debye relaxation time for water at room temperature ($\tau_{\text{D}}^{-1} = 1.4 \times 10^{11} \text{ s}^{-1}$).²⁸ This is consistent with the calculated charge densities at hydroxyl oxygen, that is, the lowest of all of the charge densities is that of the 4' oxygen of malvin (Table 2).

At the highest $[\text{H}^+]$ (fast-equilibrium regime), τ_2 tends to the sum of the forward and back reaction rates ($k_{\text{d}} + k_{\text{p}}[\text{H}^+]$), reaching a limit that is determined by our experimental resolution ($\tau_2 < 3$ ps at $[\text{H}^+] = 9.14$ M). In general, the sum of the two reciprocal decay times is equal to the sum of all four rate constants involved in the process ($1/\tau_1 + 1/\tau_2 = k_{\text{AH}^+} + k_{\text{A}} + k_{\text{d}} + k_{\text{p}}[\text{H}^+]$).²⁵ Thus, a plot of this sum against $[\text{H}^+]$ provides the value of the protonation rate constant of A^* (Table 2). Although the numerical values of the excited-state back-protonation rates, k_{p} , should be regarded with some caution due to the method (linear plots of $\lambda_1 + \lambda_2$ vs $[\text{H}^+]$) and the pH range (high concentrations of perchloric acid) used for their determination, they are similar in magnitude to those of other photoacids.²⁹

Correlation between Deprotonation Rate and Charge Density. The simplest explanation for the well-known increase in the acidity of phenols and naphthols upon excitation from the ground state to the first excited state is a decrease in the electron density at the hydroxyl oxygen and the consequent weakening

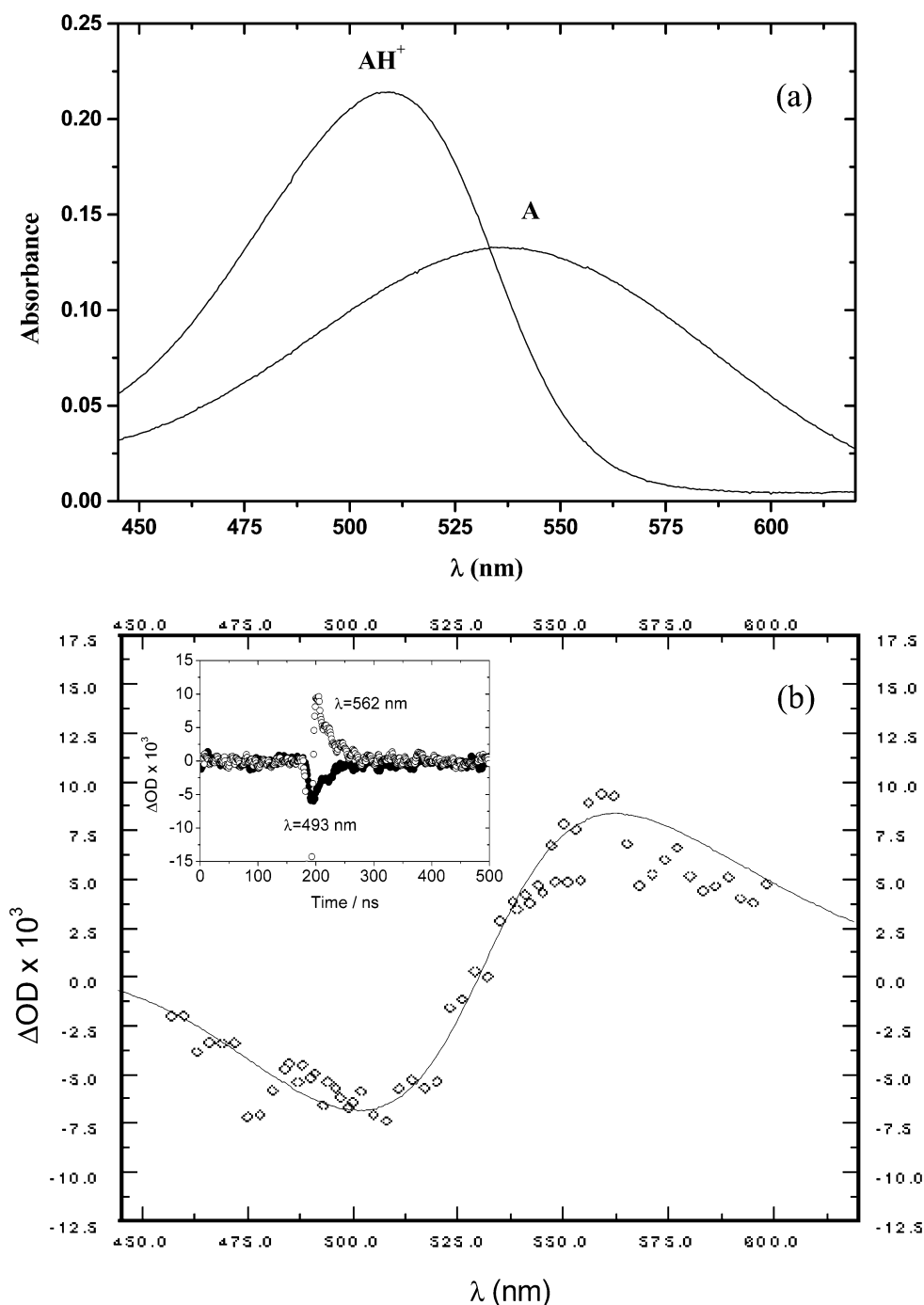


Figure 5. Absorption spectra (a) of cyanin in water at pH 0 (AH^+) and immediately after a pH jump to pH 6 (A) and (b) comparison of the differential absorption spectrum of the transient produced in an aqueous solution of cyanin at pH 2, measured immediately after the laser pulse (O) with that (—) calculated from the absorption spectra presented in panel a. The inset presents kinetic traces collected at 493 and 562 nm.

TABLE 2: Calculated Charge Densities on the Hydroxyl Oxygens, $\delta(\text{O}_7)$ and $\delta(\text{O}_4)$, Deprotonation (k_d) and Protonation (k_p) Rate Constants, and $\text{p}K_a$ of Pelargonin, Cyanin, and Malvin in the Ground and First Excited Singlet States in Aqueous Solution at 20 °C

	ground state			excited state		
	pelargonin	cyanin	malvin	pelargonin	cyanin	malvin
$\delta(\text{O}_7)$	-0.237	-0.235	-0.235	-0.221	-0.224	-0.231
$\delta(\text{O}_4)$	-0.250	-0.242	-0.240	-0.219	-0.209	-0.187
$k_d (10^6 \text{ s}^{-1})$	1.3 ± 0.8	1.8 ± 1.5	3.8 ± 1.4	4.3×10^4	4.0×10^4	1.6×10^5
$k_p (10^{10} \text{ M}^{-1} \text{ s}^{-1})$	3.6 ± 0.06	2.2 ± 0.1	2.9 ± 0.07	5.8	5.2	12
$\text{p}K_a$	4.44	4.09	3.88	0.14	0.11	-0.13

of the O—H bond. In fact, correlations between acidity constants and charge densities or electrostatic potentials at the deprotonation site are well established.³⁰

The ionic contribution to the O—H bond (E_{ionic}) is roughly proportional to the product of the charge densities on the oxygen and hydrogen atoms divided by the internuclear distance, $d_{\text{O—H}}$.

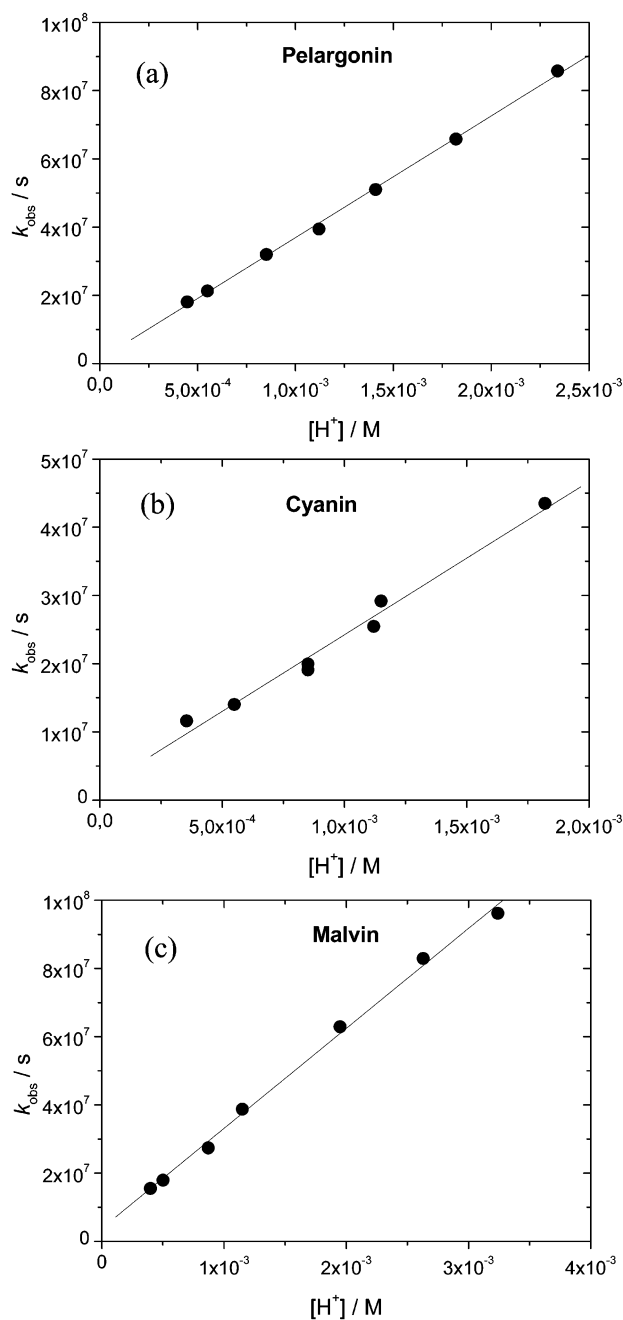


Figure 6. Laser flash photolysis determination of the dynamics of protonation and deprotonation of (a) pelargonin, (b) cyanin, and (c) malvin. The reciprocal decay time of the base is plotted as a function of $[\text{H}^+]$.

These parameters were calculated, using the AM1 semiempirical method,²³ for the ground and excited states of the three anthocyanins studied here, as well for several other compounds for which values of deprotonation rate constant are available (Table 3) or can be estimated from published pK_a values assuming diffusion control of the back-protonation.

A plot of the natural logarithm of the deprotonation rate constant vs the ionic contribution to the O–H bond is shown in Figure 7. This plot resembles the well-known Rehm–Weller plot³¹ of $\ln k$ vs ΔG° for electron transfer, having two distinct regions. At the larger values of E_{ionic} , $\ln k_d$ increases linearly with decreasing E_{ionic} , over 8 orders of magnitude of k_d . At E_{ionic} values below about 0.94, a plateau value is reached, that is, the deprotonation becomes independent of E_{ionic} . The correlation

TABLE 3: Experimental Ground- and Excited-State Deprotonation Rate Constants ($\ln k_d$), Calculated Mulliken Charge Densities for the Hydroxyl Oxygen (δ_{O}) and Proton (δ_{H}), OH Bond Length ($r_{\text{O-H}}$), and Ionic Contribution (E_{ionic}) to the O–H Bond

	δ_{O}	δ_{H}	$r_{\text{O-H}}$ (Å)	E_{ionic}^a (eV)	$\ln k_d$
Excited State					
1-naphthol	-0.251	0.241	0.9400	0.93	23.94 ^b
1-naphthol-2-sulfonate	-0.229	0.272	0.9403	0.95	22.90 ^b
1-naphthol-3,6-disulfonate	-0.272	0.225	0.9393	0.94	24.78 ^b
2-naphthol	-0.265	0.243	0.9400	0.99	18.42 ^b
2-naphthol-6-sulfonate	-0.28	0.228	0.9395	0.98	20.72 ^b
2-naphthol-6,8-disulfonate	-0.284	0.211	0.9383	0.92	23.56 ^b
2-naphthol-3,6-disulfonate	-0.258	0.2595	0.9414	1.02	20.18 ^b
8-hydroxypyrene-1,3,6-trisulfonate	-0.283	0.22	0.9391	0.95	22.80 ^c
6-bromo-2-naphthol	-0.262	0.245	0.9402	0.98	20.37 ^c
6-methyl-2-naphthol	-0.264	0.243	0.9400	0.98	16.45 ^c
7-methyl-2-naphthol	-0.267	0.243	0.9400	0.99	16.59 ^c
1-chloro-2-naphthol	-0.256	0.247	0.9394	0.97	20.01 ^c
HMF	-0.2	0.277	0.9413	0.85	25.73 ^d
DHF	-0.216	0.273	0.9413	0.90	25.11 ^e
pelargonin	-0.219	0.271	0.9410	0.91	24.48 ^f
cyanin	-0.209	0.275	0.9413	0.88	24.41 ^f
malvin	-0.187	0.286	0.9435	0.82	25.80 ^f
Ground State					
1-naphthol	-0.282	0.241	0.9399	1.04	3.69 ^g
2-naphthol	-0.28	0.238	0.9399	1.02	3.37 ^g
2-naphthol-6-sulfonate	-0.289	0.226	0.9392	1.00	4.22 ^g
2-naphthol-6,8-disulfonate	-0.304	0.227	0.9403	1.06	2.38 ^g
8-hydroxypyrene-1,3,6-trisulfonate	-0.303	0.219	0.9394	1.02	6.68 ^c
HMF	-0.239	0.27	0.9407	0.99	14.15 ^e
DHF	-0.239	0.269	0.9409	0.98	14.95 ^e
pelargonin	-0.237	0.266	0.9404	0.97	14.08 ^f
cyanin	-0.235	0.271	0.9409	0.97	14.40 ^f
malvin	-0.235	0.271	0.9409	0.97	15.15 ^f
oenin	-0.24	0.272	0.9408	1.00	15.42 ^e
<i>m</i> -bromophenol	-0.278	0.241	0.9399	1.03	2.93 ^h
<i>m</i> -methoxyphenol	-0.281	0.24	0.9395	1.03	1.50 ^h
pentachlorophenol	-0.253	0.259	0.9394	1.00	12.78 ⁱ
<i>p</i> -nitrophenol	-0.269	0.248	0.9400	1.02	7.26 ^h

^a $E_{\text{ionic}} = (\delta_{\text{O}}\delta_{\text{H}})/r_{\text{O-H}}$. ^b Reference 35. ^c Reference 29. ^d Reference 10. ^e Reference 19. ^f This work. ^g Reference 35, calculated from the pK_a value assuming k_p for excited state. ^h Reference 36, calculated from the pK_a value assuming $k_p = 2 \times 10^{10} \text{ M}^{-1} \text{ s}^{-1}$. ⁱ Reference 37, calculated from the pK_a value assuming $k_p = 2 \times 10^{10} \text{ M}^{-1} \text{ s}^{-1}$.

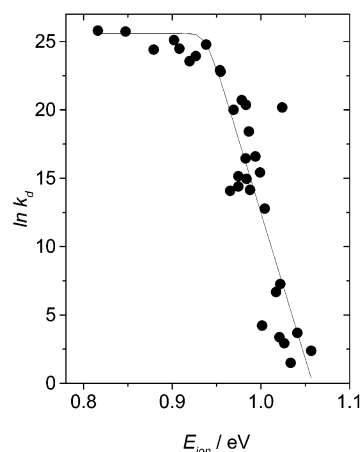


Figure 7. Correlation of deprotonation rate constants ($\ln k_d$) for ground and excited states of anthocyanins and of a series of phenols and naphthols known to be good photoacids with the calculated ionic contribution to the O–H bond (E_{ionic}). Line fitting was done with $\ln(k_d) = \ln([k_2/(k_1 + k_2)]k_1)$ and $k_1 = (\tau_D)^{-1} = 1.4 \times 10^{11} \text{ s}^{-1}$.

is surprisingly good, especially considering that it includes both the ground and excited state of neutral, anionic, and cationic acids and no consideration of solvation effects on E_{ionic} .

In a Rehm–Weller³¹ or Eigen plot,³² the *plateau* region is observed when diffusion control becomes the rate-limiting step of the reaction. However, in the case of deprotonation, translational diffusion is clearly not the limiting step because the proton acceptor, water, is the solvent and already completely surrounds the solvated molecule. It is more plausible that reorientation of water to accept or remove the leaving proton (proton solvation) is the rate-limiting step for deprotonation.³³ Indeed, the *plateau* value obtained in Figure 7 is very close to the Debye relaxation time of water (ca. 6–7 ps)²⁸ and, as pointed out by others,³⁴ must reflect the dynamics of the water reorientation that is required for the proton-transfer step to occur. In the case of *intramolecular* proton transfer, such reorientation does not play a role, and in fact, *intramolecular* proton-transfer rates faster than the 6–7 ps threshold have been observed.

Concluding Remarks

Flavylium cations of synthetic and natural anthocyanins are weak acids in the ground state and strong acids in the excited state. The deprotonation rate constants increase with the decrease of charge density on the oxygen of the hydroxyl group at which deprotonation occurs. A plot of the natural logarithm of the deprotonation rate constant vs the calculated ionic contribution to the O–H bond points to the existence of an upper limit for the rate of intermolecular proton transfer to water (6–7 ps) that must be associated with water reorientation.

Finally, the present results demonstrate that fast, adiabatic proton transfer is the predominant process responsible for the weak fluorescence of the flavylium cation form of anthocyanins. This process is highly efficient as an energy-wasting mechanism, supporting the proposal that one of the roles of anthocyanins *in vivo* is to provide plant tissues with protection from potentially deleterious excess radiant energy.

Acknowledgment. This work was partially supported by the research grants POCTI/QUI/33679/99, ICCTI/CAPES/423, and POCTI/QUI/38884/2001. A.L.M. acknowledges the Program CIENCIA (FCT, Portugal) for partial funding in the acquisition of the picosecond laser system. C.Y. acknowledges a doctoral fellowship from the Fundação de Amparo à Pesquisa do Estado de São Paulo (FAPESP). F.H.Q. thanks FAPESP for additional funding and the Conselho Nacional de Desenvolvimento Científico e Tecnológico (CNPq), Brasília, for a senior research fellowship.

References and Notes

- (1) Harborne, J. B.; Williams, C. A. *Phytochemistry* **2000**, 55, 481.
- (2) Brouillard, R. In *Anthocyanins as Food Colors*; Markakis, P., Ed.; Academic Press: New York, 1982; Chapter 9.
- (3) Meyer, A. S.; Heinonen, M.; Frankel, E. N. *Food Chem.* **1998**, 61, 71.
- (4) Satué-Gracia, M. T.; Heinonen, M.; Frankel, E. N. *J. Agric. Food Chem.* **1997**, 45, 3362.
- (5) Brouillard, R.; Dubois, J. E. *J. Am. Chem. Soc.* **1977**, 99, 1359.
- (6) Brouillard, R.; Delaporte, B. *J. Am. Chem. Soc.* **1977**, 99, 8461.
- (7) McClelland, R. A.; Gedge, S. J. *J. Am. Chem. Soc.* **1980**, 102, 5838.
- (8) Santos, H.; Turner, D. L.; Lima, J. C.; Figueiredo, P.; Pina, F.; Maçanita, A. L. *Phytochemistry* **1993**, 33, 1227.
- (9) Houbiers, C.; Lima, J. C.; Maçanita, A. L.; Santos, H. *J. Phys. Chem. B* **1998**, 102, 3578.
- (10) Lima, J. C.; Abreu, I.; Brouillard, R.; Maçanita, A. L. *Chem. Phys. Lett.* **1998**, 298, 189.
- (11) Figueiredo, P.; Lima, J. C.; Santos, H.; Wigand, M.-C.; Brouillard, R.; Pina, F.; Maçanita, A. L. *J. Am. Chem. Soc.* **1994**, 116, 1249.
- (12) Pina, F.; Benedito, L.; Melo, M. J.; Bernardo, M. A.; Parola, A. J. *J. Chem. Soc., Faraday Trans.* **1996**, 92, 1693.
- (13) Matsushima, R.; Mizuno, H.; Itoh, H. *J. Photochem. Photobiol., A: Chem.* **1995**, 89, 251.
- (14) Matsushima, R.; Mizuno, H. *Bull. Chem. Soc. Jpn.* **1994**, 67, 1762.
- (15) (a) Lima, J. C.; Danesh, P.; Figueiredo, P.; Pina, F. S.; Maçanita, A. L. *J. Photochem. Photobiol., A: Chem.* **1994**, 59, 412. (b) Figueiredo, P.; Pina, F.; Vilas-Boas, L.; Maçanita, A. L. *J. Photochem. Photobiol., A: Chem.* **1990**, 53, 411.
- (16) Furtado, P.; Figueiredo, P.; Neves, H. C.; Pina, F. *J. Photochem. Photobiol., A: Chem.* **1993**, 75, 113.
- (17) Maccarone, E.; Ferrigno, V.; Longo, M. L.; Rapisarda, R. *Ann. Chim.* **1987**, 77, 499.
- (18) Pina, F.; Melo, M. J.; Santos, H.; Lima, J. C.; Abreu, I.; Ballardini, R.; Maestri, M. *New J. Chem.* **1998**, 1093.
- (19) Maçanita, A. L.; Moreira, P. F.; Lima, J. C.; Quina, F. H.; Yihwa, C.; Vautier-Giongo, C. *J. Phys. Chem. A* **2002**, 106, 1248.
- (20) Lima, J. C. Ph.D. Thesis, Instituto Superior Técnico, Lisbon, Portugal, 1996.
- (21) Fleming, G. R.; Knight, A. W. E.; Morris, J. M.; Morrison, R. J. S.; Robinson, G. W. *J. Am. Chem. Soc.* **1977**, 99, 4306.
- (22) Striker, G.; Subramaniam, V.; Seidel, C. A. M.; Volkmer, A. *J. Phys. Chem. B* **1999**, 103, 8612.
- (23) *Hyperchem*, release 6.01 for Windows; Hypercube, Inc.: Gainesville, FL, 2000.
- (24) Lima, J. C.; Vautier-Giongo, C.; Lopes, A.; Melo, E.; Quina, F. H.; Maçanita, A. L. *J. Phys. Chem. A* **2002**, 106, 5851.
- (25) Giestas, L.; Yihwa, C.; Lima, J. C.; Vautier-Giongo, C.; Lopes, A.; Quina, F. H.; Maçanita, A. L. The Dynamics of Ultrafast Excited-State Proton Transfer in Anionic Micelles. *J. Phys. Chem. A* **2003**, ASAP article.
- (26) Birks, J. B. *Photophysics of Aromatic Molecules*; Wiley: London, 1970.
- (27) Reyes Vigil, M.; Renamayor, C. S.; Piérola, I.; Lima, J. C.; Melo, E.; Maçanita, A. L. *Chem. Phys. Lett.* **1998**, 287, 379.
- (28) Pines, E.; Magnes, B.-Z.; Lang, M. J.; Fleming, G. R. *Chem. Phys. Lett.* **1997**, 281, 413.
- (29) Arnaut, L. G.; Formosinho, S. *J. Phys. Chem.* **1988**, 92, 685.
- (30) Meek, T. L. *J. Chem. Ed.* **1992**, 69, 270.
- (31) Rehm, D.; Weller, A. *Isr. J. Chem.* **1970**, 8, 259.
- (32) Eigen, W. *Angew. Chem., Int. Ed. Engl.* **1964**, 3, 1.
- (33) Although the participation of preformed ground-state hydrogen-bonded complexes, in which water molecules are in an appropriate position for receiving the proton from the anthocyanin, cannot be excluded, intramolecular proton-transfer rates are known to exceed the 6–7 ps limit. The fact that these compounds are almost exclusively soluble in water or aqueous ethanol or methanol mixtures limits the use of solvatochromic studies to resolve this point. Nonetheless, preliminary results on the solvatochromism of the synthetic anthocyanin 7-hydroxy-4-methylflavylium (HMF) chloride have shown that the solvent-induced stabilization of the ground state (blue shift of the absorption spectrum) of HMF is proportional to the hydrogen bond donating ability of the solvent while the stabilization of the excited state (red shift of the emission spectrum) is correlated with the hydrogen bond accepting capacity of the solvent. This suggests the presence of hydrogen-bonded HMF–water complexes in both the ground and excited states. However, in the ground state, water molecules are predominantly hydrogen-bond donors to HMF, whereas in the excited state water acts predominantly as a hydrogen-bond acceptor. Thus, excitation would require rotational relaxation of the water molecules in the solvation shell of HMF prior to proton transfer.
- (34) Tolbert, L. M.; Solnetsev, K. M. *Acc. Chem. Res.* **2002**, 35, 19.
- (35) Arnaut, L. G.; Formosinho, S. *J. Photochem. Photobiol., A: Chem.* **1993**, 75, 1.
- (36) Albert, A.; Serjeant, E. P. *The Determination of Ionization Constants: A Laboratory Manual*, 3rd ed.; Chapman and Hall: New York, 1984; p 145.
- (37) Worthing, C. R.; Walker, S. B. *The Pesticide Manual, A World Compendium*, 8th ed.; British Crop Protection Council: London, England, 1987; p 641.